

**Large- p_T Inclusive π^0 Cross Sections
and Next-to-Leading-Order QCD Predictions**

P. Aurenche,¹ M. Fontannaz,² J.-Ph. Guillet,¹ B. A. Kniehl,³ M. Werlen¹

¹ Laboratoire d'Annecy-le-Vieux de Physique Théorique LAPTH,
B.P. 110, F-74941 Annecy-le-Vieux Cedex, France

² Laboratoire de Physique Théorique,* Université de Paris XI,
Bâtiment 210, F-91405 Orsay Cedex, France

³ II. Institut für Theoretische Physik, Universität Hamburg,
Luruper Chaussee 149, D-22761 Hamburg, Germany

Abstract

We review the phenomenology of π^0 production at large transverse momentum in proton-induced collisions. Uncertainties in the next-to-leading-order predictions of Quantum Chromodynamics are discussed. The comparison with data reveals that the disagreement between theory and experiment lies essentially in an overall normalization factor. The situation for π^0 production is contrasted with that of prompt-photon production in hadronic collisions.

hep-ph/9910252
LAPTH-751/99
LPT-Orsay/99/78
DESY 99-153
October 1999

*Unité mixte de recherche (CNRS) UMR 8627

1 Introduction

The production of hadrons at large transverse momentum p_T (in hadron-hadron or hadron-photon collisions) offers a classical test of perturbative QCD. The cross sections of the hard subprocesses are calculated with next-to-leading-order (NLO) accuracy [1], the quark and gluon distributions in the initial hadrons are measured in deep-inelastic-scattering experiments [2,3,4,5] and the fragmentation functions describing the transitions of the partons into the final-state hadrons are extracted from e^+e^- -annihilation data [6,7,8]. Therefore, all the building blocks of the large- p_T cross sections are in principle known, and the comparison with data provides interesting tests of the theory.

The hadroproduction of large- p_T π^0 mesons has been studied by the CGGRW Collaboration [6], who obtained good agreement between the QCD predictions and collider π^0 cross sections. On the other hand, fixed-target data with a lower center-of-mass energy \sqrt{s} ($23 \text{ GeV} \lesssim \sqrt{s} \lesssim 30 \text{ GeV}$) overshoot the theoretical predictions, and it was impossible to obtain an overall agreement with all the large- p_T π^0 data. Large- p_T charged-hadron cross sections were studied in hadroproduction at collider energies [9] and in photoproduction at HERA energies [7]. In that case, reasonable agreement between theory and data was reached, but one must remember that these predictions are sensitive to the choice of the factorization and renormalization scales in the p_T -range which was studied ($p_T \lesssim 10 \text{ GeV}$).

In this paper, we come back to the study of the large- p_T π^0 cross sections. New fixed-target data appeared recently [10,11], completing those already available in the range $23 \lesssim \sqrt{s} \lesssim 30 \text{ GeV}$ [12]. On the theoretical side, new sets of fragmentation function extracted from LEP data are now available [7]. One must also notice that $\Lambda_{\overline{\text{MS}}}^{(4)}$ has increased from $\sim 200 \text{ MeV}$ to $\sim 300 \text{ MeV}$ since the time of the first study [6]. This new value of $\Lambda_{\overline{\text{MS}}}$ gives rise to a non-negligible increase of the QCD cross section in the p_T range studied here ($p_T \lesssim 10 \text{ GeV}$).

Another important reason for this study is the publication of new data on prompt-photon cross sections [10,11]. A recent QCD analysis of all fixed-target and ISR data [13] leads to the conclusion that theory is in reasonable agreement with experiment, with the exception of two data sets, as shown in Fig. 1. However, it should be remembered that the comparison with QCD predictions can only be done for high-enough values of p_T (*e.g.* $p_T \gtrsim 5 \text{ GeV}/c$ for the E706 and ISR energy ranges), where the scale dependence of the theoretical cross sections is not too large. Therefore, in Fig. 1, one should not consider the

first points of the E706 and ISR experiments. The introduction of an additional intrinsic transverse momentum k_T of the incoming partons, strongly advocated in Refs. [10,14] to enforce agreement between QCD predictions and experiment, is not a very satisfactory solution; the agreement with the E706 data sets is improved, but the agreement with other data sets is reduced.

This situation is challenging and leads us to look at large- p_T π^0 production. The large- p_T π^0 mesons form a significant background for the prompt photons, and their cross section must be carefully measured in order to allow for a reliable estimate of the “fake prompt photons,” in particular due to configurations in which one photon from the decaying π^0 escapes detection. Therefore, there is a strong experimental correlation between the prompt-photon and the π^0 cross sections, especially at low p_T values, where the π^0 background is largest. A study of the latter could bring some clarification on the prompt-photon puzzle.

Section 2 of this paper is devoted to a discussion of the theoretical calculation of the π^0 cross sections. We emphasize the uncertainties associated with the QCD scales, the determination of the fragmentation functions and the importance of the higher-order (HO) corrections. We discuss the comparison of theoretical predictions with data at fixed-target energies in section 3 and with data at higher energies in section 4. Section 5 contains the conclusions.

2 Theoretical Framework

At NLO, the inclusive cross section for the hadroproduction of a single hadron h , differential in the transverse momentum p_T and the pseudorapidity η of h , takes the following form:

$$\begin{aligned} \frac{d\sigma^h}{d\vec{p}_T d\eta} = & \sum_{i,j,k=q,g} \int dx_1 dx_2 F_{i/h_1}(x_1, M) F_{j/h_2}(x_2, M) \frac{dz}{z^2} D_k^h(z, M_F) \\ & \times \left[\left(\frac{\alpha_s(\mu)}{2\pi} \right)^2 \frac{d\hat{\sigma}_{ij,k}}{d\vec{p}_T d\eta} + \left(\frac{\alpha_s(\mu)}{2\pi} \right)^3 K_{ij,k}(\mu, M, M_F) \right]. \end{aligned} \quad (1)$$

The parton densities of the incoming hadrons h_1 and h_2 are given by F_{i/h_1} and F_{j/h_2} ; the fragmentation of a parton k into the hadron h is described by the fragmentation function $D_k^h(z, M_F)$; $d\hat{\sigma}_{ij,k}/d\vec{p}_T d\eta$ is the Born cross section of the subprocess $i+j \rightarrow k+X$; and $K_{ij,k}$ is the corresponding HO correction term. In this paper, we shall use the ABFOW

[2], CTEQ [3,4] and MRST [5] parton densities. For the fragmentation functions, we shall use the parametrization of Ref. [7]. These fragmentation functions were derived from fits to charged-pion spectra, but we make the usual assumption, supported by data, that the rate of π^0 production is half of that for charged pions. They are preferable to the parametrizations of Ref. [6], which predate the publication of the LEP hadronic spectra.

Expression (1) depends on the initial- and final-state factorization scales, M and M_F , and on the renormalization scale μ . The cross section $d\sigma^h/d\vec{p}_T d\eta$, calculated to all orders in α_s , is independent of M , M_F and μ . However, the perturbative series calculated at fixed order in α_s does depend on these scales, the compensation between the variations of $F_{i/h_1}(M)$, $F_{j/h_2}(M)$, $D_k^h(M_F)$ and $\alpha_s(\mu)$ and those of $K_{ij,h}(\mu, M, M_F)$ being incomplete. Therefore, we shall carefully explore the scale dependence of the cross section (1). On the one hand, we shall use “standard scales” $M = M_F = \mu = p_T/\kappa$, with κ varying around $\kappa = 2$, and, on the other hand, we shall fix the scales by using the Principle of Minimum Sensitivity (PMS) [15],

$$\mu \frac{\partial}{\partial \mu} \frac{d\sigma^h}{d\vec{p}_T d\eta} = M \frac{\partial}{\partial M} \frac{d\sigma^h}{d\vec{p}_T d\eta} = M_F \frac{\partial}{\partial M_F} \frac{d\sigma^h}{d\vec{p}_T d\eta} = 0, \quad (2)$$

which determines the optimal scales μ_{opt} , M_{opt} and $M_{F,\text{opt}}$. An illustration of the scale sensitivity is presented in Fig. 2, where the differential cross section for the inclusive production of single π^0 mesons, with $p_T = 7$ GeV/c and $|\eta| < 0.75$, through the scattering of 530 GeV/c protons on a fixed Beryllium target is considered. Specifically, the contours of constant cross section are shown in the (M, M_F) plane. For each set (M, M_F) , μ is determined by the first equality in Eq. (2). As expected, one finds a minimum, corresponding to the optimal choice defined by Eq. (2), but one also notices that the area of stability under changes of scales around this optimal point is not very large. It is smaller than in the case of prompt-photon production. We noticed in several numerical studies that it is not possible to verify the PMS criterion (2) for too small values of p_T , typically for $p_T \lesssim 5$ GeV/c. This indicates that the HO corrections are large and that the QCD predictions are quite unstable under changes of scales. Therefore, we shall emphasize the comparison between theory and experiment at $p_T \gtrsim 5$ GeV/c, although we shall also explore smaller p_T values.

Since working in the optimal scheme is rather cumbersome and requires a lot of numerical work, we compare, in general, theory predictions for fixed scales with experiment. We use the standard choices $M = M_F = \mu = p_T/2$ and $p_T/3$. As will be discussed later, the optimal scales, derived from Eq. (2), turn out to interpolate between these two choices,

depending on the kinematical range considered.

Besides the scale dependence, there are other sources of uncertainties in Eq. (1), which come from the parton densities and the fragmentation functions. The parton densities are generally determined with good accuracy. However, at small p_T and for scale $p_T/3$, the factorization scale may approach the starting scale Q_0 of the QCD evolution. In this region, the parton densities are not constrained by data. To avoid this problem when using the scale $p_T/3$, we thus require p_T to be larger than 4.5 GeV/c.

Another source of uncertainty concerns the fragmentation functions. The quark fragmentation is now well constrained by PETRA, PEP and LEP data [7,8]. However, the dominant support to Eq. (1) comes from the large- z domain, where the e^+e^- data are scarce. For instance, numerical studies of Eq. (1) indicate that the mean z value is about 0.85 for $4 < p_T < 8$ GeV/c and $\sqrt{s} = 31$ GeV. There are very few data points in the range $0.8 < z < 1$ (zero or one point in most data sets), and they have large error bars. Therefore, we expect the uncertainty coming from the fragmentation functions to be of the order of a few tens of percents. It must also be noticed that the gluon fragmentation function is not well determined by e^+e^- data, since it appears there only at NLO. More constraints could, in principle, be obtained from inclusive pion production at large transverse momentum in hadronic collisions. For example, the inclusive large- p_T charged-hadron cross section has been measured by the UA1 Collaboration [16] in the range $5 \lesssim p_T \lesssim 20$ GeV/c. These data are compatible with the parametrization of Ref. [7], but they are also compatible with the same parametrization after the normalization of the gluon fragmentation function has been increased by 30% to 40%. (Such a large change in the gluon fragmentation function is still compatible with the e^+e^- data.) This gives us an estimate of the flexibility in the gluon parametrization. We remark that changing the gluon fragmentation function may affect the slope of the p_T distributions, since the low x_T regions will be more strongly affected. Besides these problems related to the z behavior of the fragmentation functions, we should remark that we are led to explore small fragmentation scales (in particular, when using $M_F = p_T/3$) far away from the kinematical regions where the fits are performed. In summary, hadronic data require large z values and small scales, while the fragmentation functions are (mostly) extracted from e^+e^- data at medium z values and large scales.

Finally, let us mention that we do not use theoretical expression in which the large $\ln(1 - z)$ terms present in the HO corrections are resummed [17,18]. Indeed, in order to be coherent, one should also use resummed expressions when extracting fragmentation

functions from e^+e^- data. Such an analysis has not been done so far. It would certainly be very interesting to pursue phenomenological studies in this direction [19]. One must, however, keep in mind that the optimization procedure of Stevenson and Politzer [15] amounts to a partial resummation of the $\ln(1-z)$ terms [20].

For all these reasons, we do not expect a very good agreement between fixed-target data and QCD predictions. The expected agreement should only be within a few tens of percent. At larger energies, the mean value of z is smaller and the sensitivity to the scale variations is reduced. A better agreement is therefore expected and has been verified in previous studies [6,9]. This point will be discussed later.

In this paper, all the calculations are performed in the $\overline{\text{MS}}$ scheme. The value of $\Lambda_{\overline{\text{MS}}}$ in α_s , calculated at two loops, is taken to be equal to the one used in the parton densities.

3 Fixed-Target Data and Theory

3.1 Inclusive Distributions in p_T

The data that we are going to discuss are displayed in Fig. 3. Unlike what was observed in the case of prompt-photon production, the π^0 data taken at the same energy are quite compatible with each other, with the exception of ISR data at $\sqrt{s} = 63$ GeV, where the R806 [21] and AFS [22] data disagree for $p_T \lesssim 6$ GeV/c. The increase in cross sections as \sqrt{s} increases at fixed p_T is also visible. Let us emphasize that we only consider pp , $p\bar{p}$ and pBe data in order to reduce the uncertainties due to the parton densities of the incoming hadrons. We do not study πp data, but concentrate on proton-induced fixed-target data and ISR data in the energy range below $\sqrt{s} = 63$ GeV.

In what follows, we consider only the range $p_T > 4$ GeV/c, which is covered by almost all data sets. With this cut, we also efficiently suppress possible non-perturbative contributions to the cross sections, such as power corrections, intrinsic k_T effects, *etc.*

In Fig. 4, we show the effects of the variation in the parton densities and scales on the predictions for the WA70 experiment [12]. For both scale choices, $p_T/2$ and $p_T/3$, we observe the following hierarchy: ABFOW and CTEQ5M lead to the smallest and largest predictions, respectively, while MRST2 leads to an intermediate result. The result for CTEQ4M almost coincides with that for MRST2 and is not shown in Fig. 4. This hierarchy may be explained by the different $\Lambda_{\overline{\text{MS}}}$ values used in the evaluations of α_s . For four quark flavors, these are 230 MeV for ABFOW, 296 MeV for CTEQ4M, 300 MeV

for MRST2 and 326 MeV for CTEQ5M. When α_s is evaluated with a common value of $\Lambda_{\overline{\text{MS}}}$, the four results become very similar. The effect of the scale choice is also clearly displayed. One notices a p_T -independent increase by roughly a factor of two when the scale is reduced from $p_T/2$ to $p_T/3$. This is a typical example for the sensitivity of the theory to the scale choice. As we shall see later, the results obtained using optimal scales are close to those obtained with scale $p_T/3$. As expected, the agreement between data and theory is not very good. With small scales ($\sim p_T/3$), the theory underestimates the data by some 40% to 50%. In Fig. 5, UA6 pp data [11] are compared with the corresponding QCD predictions. For this experiment, the QCD predictions for scale $p_T/3$ undershoot the data by some 30%.

Similar remarks hold for the E706 data [10]. In Fig. 6, we display data and predictions for $\sqrt{s} = 31.6$ GeV. One observes that the curve corresponding to the optimal scales (labelled PMS) is very close to the one obtained with scale $p_T/3$. Here again, the disagreement between theory and data, for scale $p_T/3$ or optimal scales, is of the order of a few tens of percents. It is interesting to notice that, with scale $p_T/2$, which allows one to extend the predictions down to smaller values of p_T , the theoretical cross section is almost parallel to the data. Therefore, there is no such increase of the ratio of data over theory as was observed in the prompt-photon case (see Fig. 1). Very similar conclusions can be drawn from the comparison of the E706 data at $\sqrt{s} = 38.8$ GeV with theory.

Finally, in Fig. 7, we show the ISR R806 data at $\sqrt{s} = 30.6$ GeV [21] and the theoretical predictions obtained with scales $p_T/2$ and $p_T/3$. Here again, small scales lead to the best agreement with the data.

From this short survey of data and QCD predictions we can draw some preliminary conclusions. As expected, we do not obtain a very good agreement with respect to normalization. The predictions for scale $p_T/3$ systematically underestimate the data by some 30% to 50% for all considered experiments. On the other hand, the p_T behavior is well reproduced. One also notices that all data appear to be consistent with each other.

3.2 Inclusive Distributions in x_T

The above discussion is best summarized by displaying on a linear scale the data as differential cross sections in x_T normalized to the theoretical predictions. The data, normalized to the NLO predictions evaluated using set MRST2 and a common scale set equal to $p_T/2$, are displayed in Figs. 8 and 9. We notice that the normalized data are mutually

compatible within $\pm 20\%$, and that multiplying the theoretical predictions by a common normalization factor of 2.5 will bring data and theory in reasonable agreement. It is also interesting to remark that the ratio of data over theory is rather flat and shows no such sharp rise at low x_T as was observed in the prompt-photon production experiments (see Fig. 1).

These general features are also found when comparing data and theory with the common scale put equal to $p_T/3$. The results are shown in Figs. 10 and 11 for the MRST2 parton distributions. The major difference between theory and experiment now resides in a normalization factor of about 1.45. Comparing Fig. 11 with Fig. 9, one notices the different slope of the data-over-theory ratio at small x_T values, corresponding to $p_T \lesssim 5$ GeV/c, indicating that the theoretical predictions are rather unstable in this region and cannot be trusted.

3.3 Discussion

Based on the above analysis of fixed-target data (WA70, UA6, E706, R806 at $\sqrt{s} = 30.6$ GeV), we reach the following conclusions concerning inclusive single- π^0 production. All data appear to be consistent with each other to within $\pm 20\%$. However, they differ from the fixed-scale theoretical predictions by a rather large normalization factor, namely $K = 2.5 \pm 0.5$ for scale $p_T/2$ and $K = 1.45 \pm 0.25$ for scale $p_T/3$. In the latter case, it is worth investigating if this normalization factor could be accounted for, in the theoretical calculations, by a different choice of fragmentation functions, which are still rather flexible in the kinematical range of interest, as explained in section 2.

This situation is to be compared to that of prompt-photon production, where the scattering of data sets is much larger. In fact, normalized to the theoretical predictions for fixed scales, the measured E706 rate at $\sqrt{s} = 31.6$ GeV appears two to four times larger than the corresponding WA70 rate.

Another feature distinguishes the π^0 spectra from the prompt-photon spectra when they are compared to theory. For scale $p_T/2$, the data-over-theory ratio for the π^0 data is rather flat down to rather low x_T values (see Fig. 9), while the corresponding ratio for the prompt-photon data is found to exhibit a sharp rise for decreasing x_T . For scale $p_T/3$, a rise is observed for both π^0 and prompt-photon data, the rise being sharper in the latter case. This change of behavior signals an instability of the theory: for π^0 production at E706 energies, a change of scales introduces a change of slope in the p_T spectrum. For WA70

or UA6 energies, the change of scales reduces to a change in the overall normalization.

A final remark concerns the energy variation of the π^0 spectrum. By comparing data at different energies in the very same experiment, we are able to better examine the variation with \sqrt{s} of the theoretical predictions. This can be done by looking at Figs. 9 and 11, where E706 data at $\sqrt{s} = 31.6$ GeV and 38.8 GeV are displayed. We notice a 30% to 40% difference in normalization, which could indicate that the theoretical predictions calculated with fixed scales are not able to follow the energy dependence of the data. The use of optimized scales does not improve the agreement with data, since the predictions based on scale $p_T/3$ or optimized scales give very similar results for all data with energy below $\sqrt{s} \approx 40$ GeV.

4 Higher-Energy Data and Theory

In Fig. 12, we compare two sets of ISR data at 63 GeV, from the R806 [21] and AFS [22] Collaborations, with theoretical predictions. In contrast to the results for lower energies, we observe a remarkable stability in the theoretical predictions for $p_T \gtrsim 5$ GeV/c ($x_T \gtrsim 0.16$): all our scale choices lead to similar predictions. Below $p_T \approx 5$ GeV/c, the predictions diverge. The choice $p_T/2$ and the use of optimized scales give similar results, while the choice $p_T/3$ leads to a cross sections which is smaller by a factor of two. Below $p_T \approx 6$ GeV/c, no conclusion is possible because each data set favours a different scale choice. Given the statistical relevance of the R806 data, the choice $p_T/2$ or the use of optimized scales appear to be most appropriate.

The agreement of theory with both data sets is rather good for $p_T \gtrsim 6$ GeV/c, although the theoretical expectations tend to be somewhat higher than the data, a situation which is different from the fixed-target case. This fact may be related to the observation made above concerning the energy variation of the data-over-theory ratio. This can be checked, to an extent which is limited by the relatively large error bars, by comparing the fixed-scale theory to the three sets of R806 data at $\sqrt{s} = 30.6, 44.8$ and 62.8 GeV. We find that, at fixed x_T , this ratio tends to decrease when the energy increases, in agreement with the E706 results.

Turning to the UA1 data on charged-pion production [16], similar comments as above can be made. The theoretical predictions at large p_T values, above $p_T \approx 7$ GeV/c, are relatively stable and agree well with the data, while, at lower p_T values, the predictions

start to diverge, thus bracketing the experimental points.

5 Conclusions

The fairest conclusion to be drawn from our studies of pion production in hadronic collisions is that the phenomenology of this process is not yet completely understood! Several problems can be identified.

On the theoretical side, the main difficulty lies in the scale instability, which is significant at low energy but disappears for $\sqrt{s} \gtrsim 60$ GeV, at least for large-enough p_T values. Hopefully, this instability will be partly removed by resumming the large $\ln(1-z)$ terms associated with the fragmentation process, very much in the way the resummation of threshold factors improved the predictions of prompt-photon production at large transverse momentum [17,18,19]. This improvement would be important in order to better understand the energy dependence of the cross sections, which, as we have seen, cannot be fully understood when using the fixed-scale approach. In the meantime, the choice of optimized scales, which is equivalent to setting the scales equal to $p_T/3$ at fixed-target energies and to $p_T/2$ at upper ISR energies, seems to be the most appropriate one and is anticipated to give results not too far from the resummed theory (*cf.* the case of prompt-photon production).

On the phenomenological side, one needs a second generation of fragmentation functions, based on the resummed approach and also taking account of pion spectra in (selected) hadronic collisions. From the e^+e^- data, upon which existing parametrizations are based, the gluon to pion fragmentation is largely undetermined, and there are very few experimental points to directly constrain the quark to pion fragmentation at very large z values. There is probably enough flexibility in the fragmentation functions to change the size of the predictions for hadronic collisions by 30% or so. This point is certainly worth a more detailed investigation.

Comparing theory with data, the fixed-target data are found to lie systematically above the theory predictions, while the ISR data are compatible with or somewhat below the predictions and the UA1 data are in perfect agreement with the predictions. This problem of energy dependence of the cross section at fixed x_T is particularly manifest in the case of the E706 data. Is this an experimental problem? Is the scale dependence of the theory more involved than expected? Redoing the phenomenology using the resummed approach

will probably help to better understand this point.

Although confused, the case of π^0 production is still much simpler than that of prompt-photon production, where 24 GeV and 63 GeV data are rather compatible with the predictions, while 30 GeV and 40 GeV data are much larger. Considering only experiments below 40 GeV and taking into account the fact that the π^0 data taken in those experiments are compatible with each other, this seems to indicate that the systematic errors on prompt-photon production are probably underestimated. In particular, the background subtraction necessary to obtain the prompt-photon spectrum should be carefully re-assessed.

It is important for the search of the Higgs-boson decay to two photons to understand the production of photons and pions at LHC energies. Given the confused situation at lower energies, after more than twenty years of intense experimental and theoretical efforts, a lot of work remains to be done to achieve this goal.

References

- [1] F. Aversa, P. Chiappetta, M. Greco, J.-Ph. Guillet, Phys. Lett. **B210** (1988) 225, **B211** (1988) 465; Nucl. Phys. **B327** (1989) 105.
- [2] ABFOW Collaboration, P. Aurenche *et al.*, Phys. Rev. **D39** (1989) 3275.
- [3] CTEQ Collaboration, H. L. Lai *et al.*, Phys. Rev. **D55** (1997) 1280.
- [4] CTEQ Collaboration, H. L. Lai *et al.*, Report No. MSU-HEP-903100, hep-ph/9903282 (March 1999).
- [5] A. D. Martin, R. G. Roberts, W. J. Stirling, R. S. Thorne, Eur. Phys. J. **C4** (1998) 463; Report No. DTP/99/64, OUTP/9931P, RAL-TR-199-047, hep-ph/9907231 (July 1999).
- [6] P. Chiappetta, M. Greco, J.-Ph. Guillet, S. Rolli, M. Werlen, Nucl. Phys. **B412** (1994) 3.
- [7] J. Binnewies, B. A. Kniehl, G. Kramer, Z. Phys. **C65** (1995) 471; Phys. Rev. **D52** (1995) 4947.
- [8] L. Bourhis, M. Fontannaz, J.-Ph. Guillet, M. Werlen, in preparation.

- [9] F. M. Borzumati, G. Kramer, Z. Phys. **C67** (1995) 137; B. A. Kniehl, Proceedings of the Ringberg Workshop on New Trends in HERA Physics, Tegernsee, Germany, 25-30 May 1997, edited by B. A. Kniehl, G. Kramer, A. Wagner.
- [10] E706 Collaboration, L. Apanasevich *et al.*, Phys. Rev. Lett. **81** (1998) 2642.
- [11] UA6 Collaboration, G. Balocchi *et al.*, Phys. Lett. **B436** (1998) 222.
- [12] WA70 Collaboration, M. Bonesini *et al.*, Z. Phys. **C38** (1988) 371.
- [13] P. Aurenche, M. Fontannaz, J. Ph. Guillet, B. Kniehl, E. Pilon, M. Werlen, Eur. Phys. J. **C9** (1999) 107.
- [14] CTEQ Collaboration, L. Apanasevich *et al.*, Phys. Rev. **D59** (1999) 074007.
- [15] P. M. Stevenson, Phys. Rev. **D23** (1981) 2916; P. M. Stevenson, H. D. Politzer, Nucl. Phys. **B277** (1986) 758; P. Aurenche, R. Baier, M. Fontannaz, D. Schiff, Nucl. Phys. **B286** (1987) 509.
- [16] UA1 Collaboration, G. Bocquet *et al.*, Phys. Lett. **B366** (1996) 434.
- [17] E. Laenen, G. Oderda, G. Sterman, Phys. Lett. **B438** (1998) 173.
- [18] S. Catani, M. L. Mangano, P. Nason, JHEP **9807** (1998) 024.
- [19] S. Catani, M. L. Mangano, P. Nason, C. Oleari, W. Vogelsang, JHEP **9903** (1999) 025.
- [20] P. Aurenche, R. Baier, M. Fontannaz, Z. Phys. **C48** (1990) 143.
- [21] R806 Collaboration, C. Kourkouvelis *et al.*, Z. Phys. **C5** (1980) 95.
- [22] AFS Collaboration, E. Anassontzis *et al.*, Sov. J. Nucl. Phys. **51** (1990) 836 [Yad. Fiz. **51** (1990) 1314].

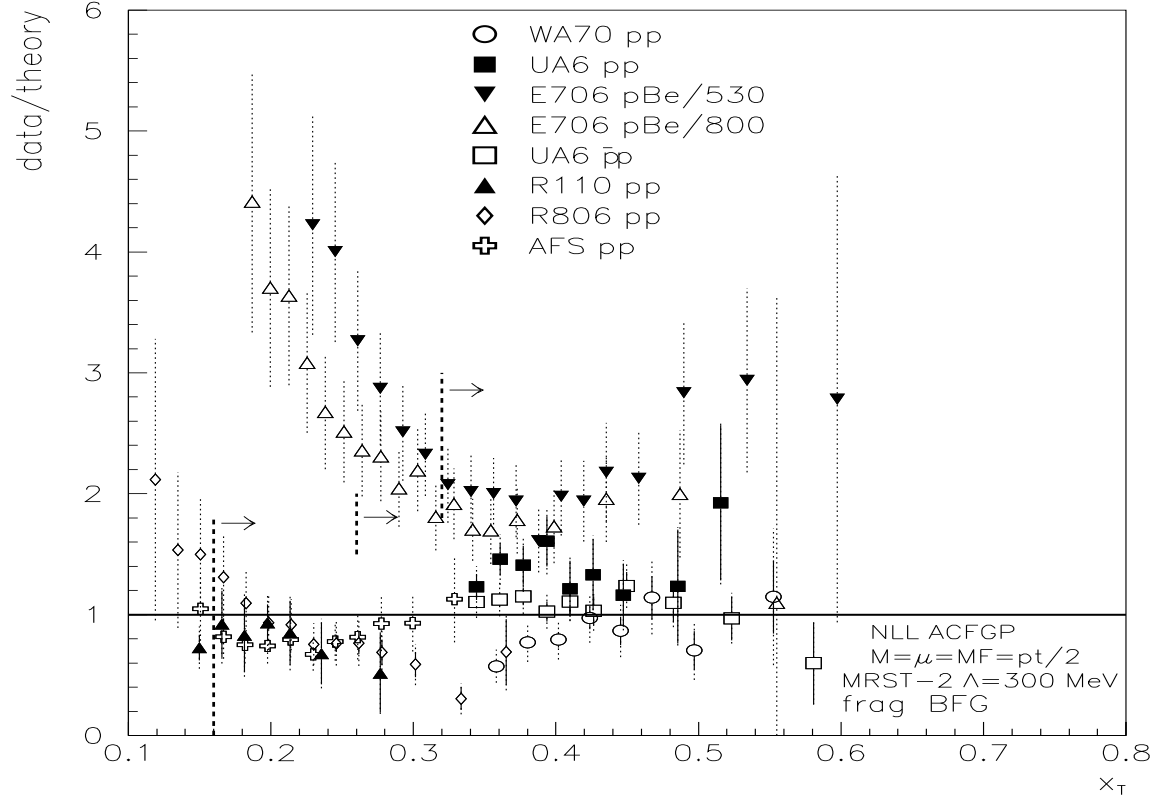


Figure 1: *Dependence on x_T of experimental cross sections for inclusive prompt-photon production normalized to NLO predictions based on the MRST2 [5] parton densities. The dotted vertical lines correspond to $p_T = 5$ GeV/c for the E706 and ISR experiments.*

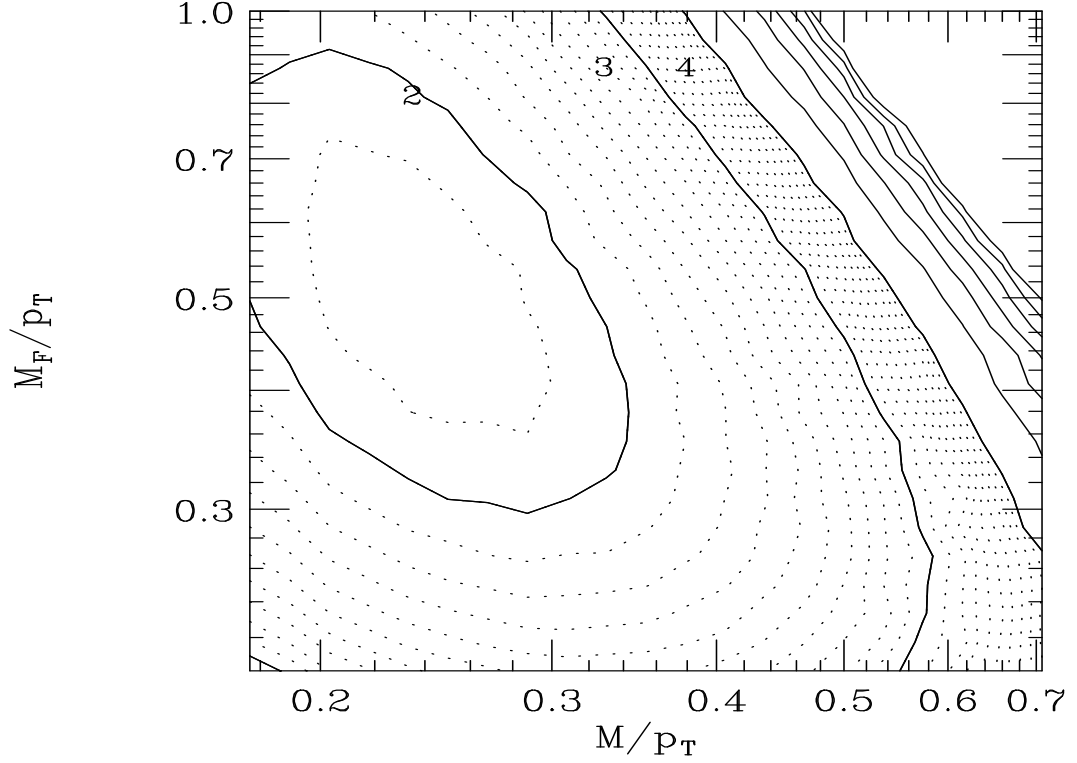


Figure 2: *Differential cross section $Ed^3\sigma/d^3p$ for the inclusive production of π^0 mesons with $p_T = 7$ GeV and $|\eta| < 0.75$ in the scattering of 530 GeV protons on a fixed Beryllium target, evaluated as a function of the initial-state factorization scale M and the fragmentation scale M_F using the MRST2 [5] parton densities. The contours of constant cross section are shown in the (M, M_F) plane. At each point, the renormalization scale μ is evaluated from Eq. (2).*

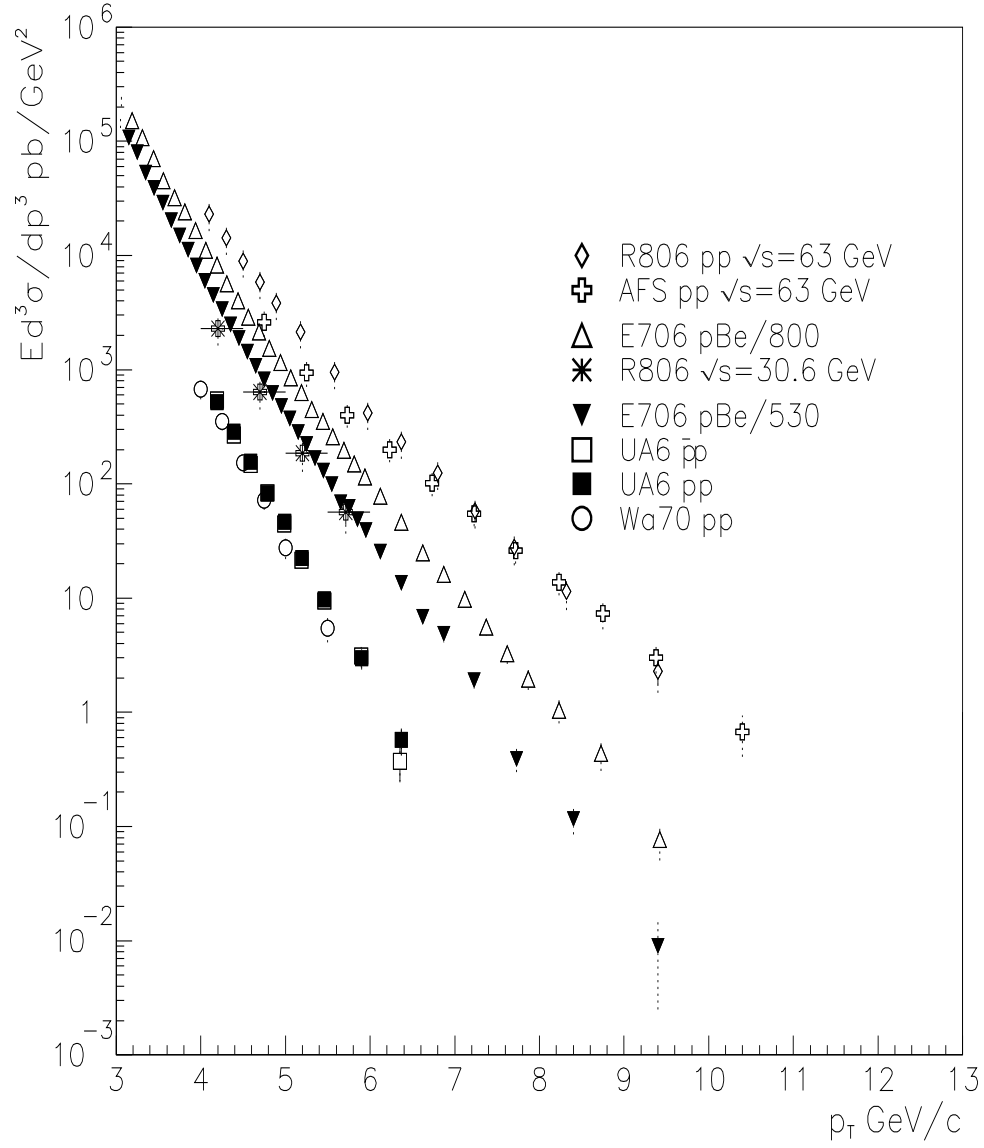


Figure 3: *Compilation of the inclusive π^0 cross sections discussed in the text as functions of p_T .*

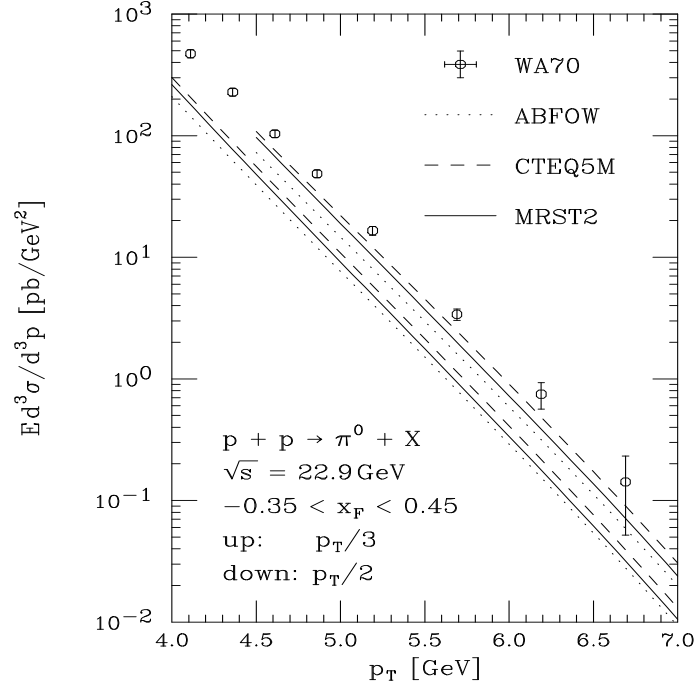


Figure 4: Comparison of WA70 [12] π^0 data with NLO predictions for three different sets of parton densities and two different scale choices. The statistical and systematic errors are added in quadrature.

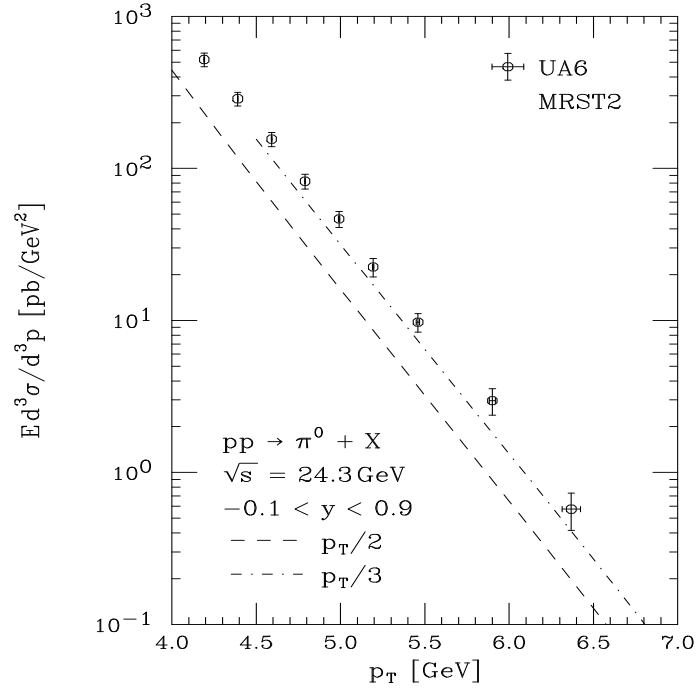


Figure 5: Comparison of UA6 [11] π^0 data with NLO predictions based on the MRST2 [5] parton densities. Very similar results are obtained with the CTEQ4M [3] parton densities.

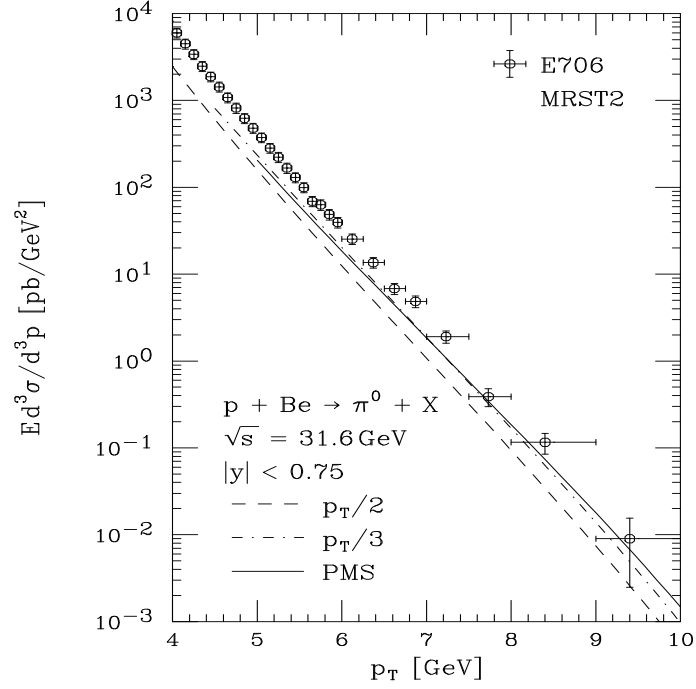


Figure 6: Comparison of E706 [10] π^0 data at $E = 530 \text{ GeV}$ with NLO predictions based on the MRST2 [5] parton densities.

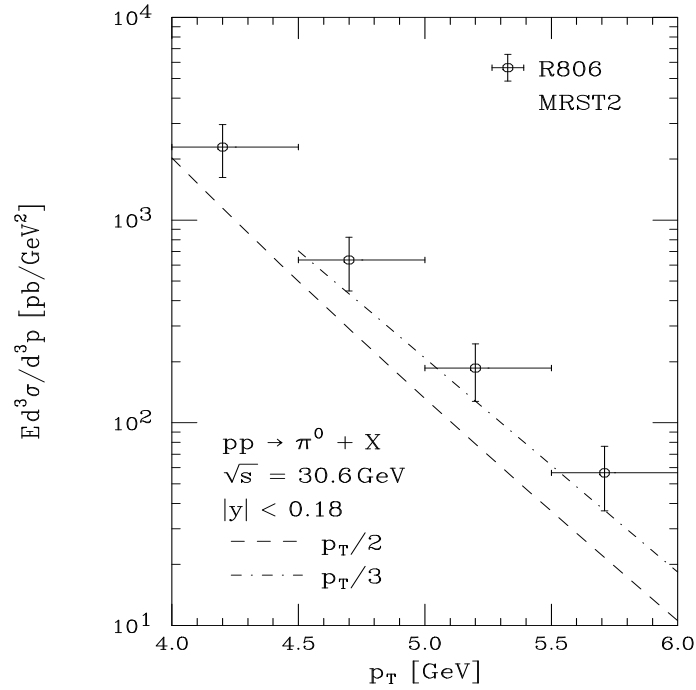


Figure 7: Same as Fig. 5, but for R806 [21] π^0 data at $\sqrt{s} = 30.6 \text{ GeV}$.

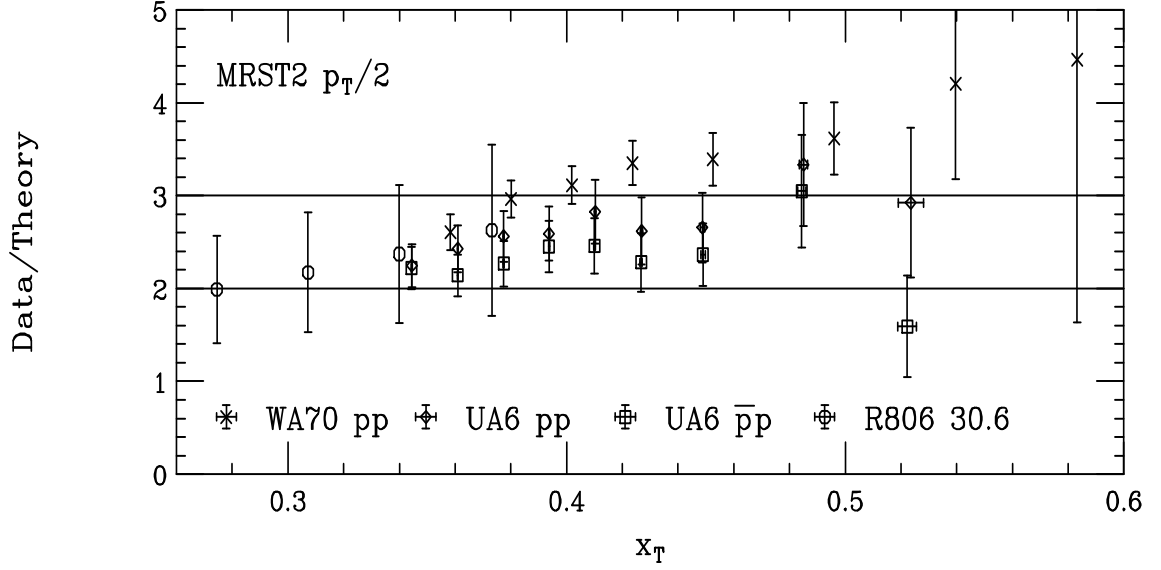


Figure 8: Comparison of WA70 [12], UA6 [11] and ISR [21] π^0 data with NLO predictions based on the MRST2 [5] parton densities. All scales are set equal to $p_T/2$ with $p_T = 2x_T\sqrt{s}$. The horizontal lines drawn at 2 and 3 illustrate the mutual agreement of all data sets to within $\pm 20\%$.

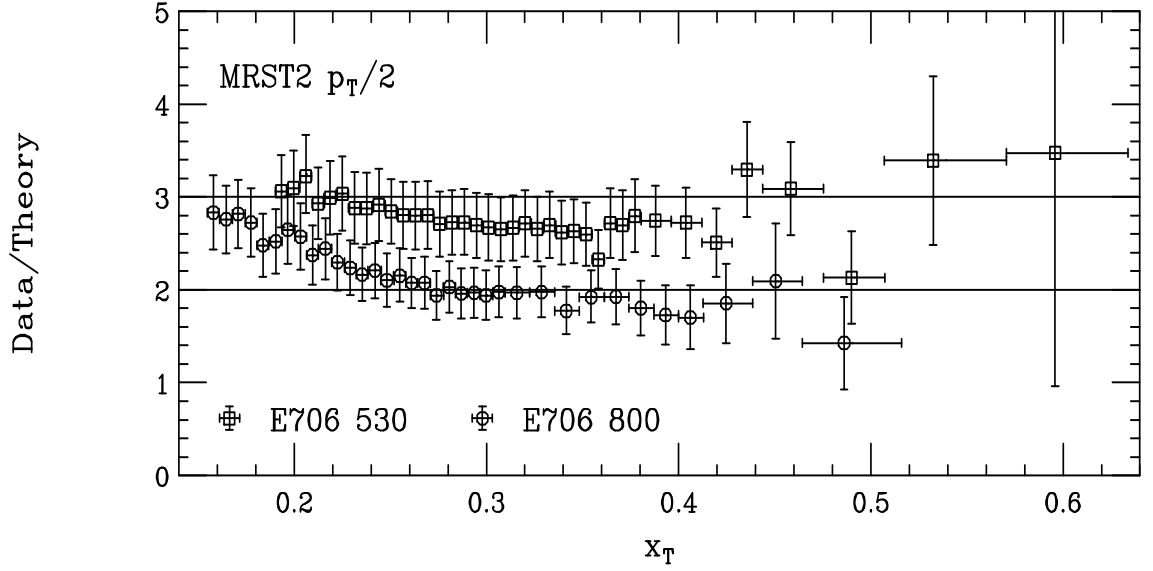


Figure 9: Same as Fig. 8, but for E706 [10] π^0 data.

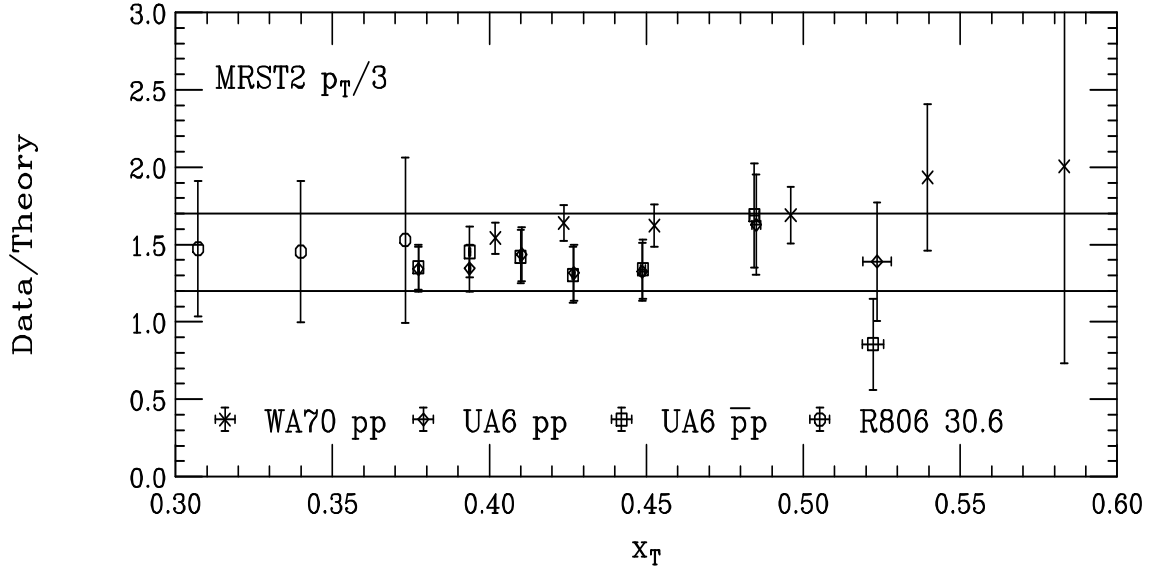


Figure 10: Same as Fig. 8, but for scale choice $p_T/3$. The horizontal lines drawn at 1.2 and 1.7 illustrate the mutual agreement of all data sets to within $\pm 20\%$. Only data points with $p_T > 4.5$ GeV are kept to avoid the use of too small factorization scales in the NLO predictions.

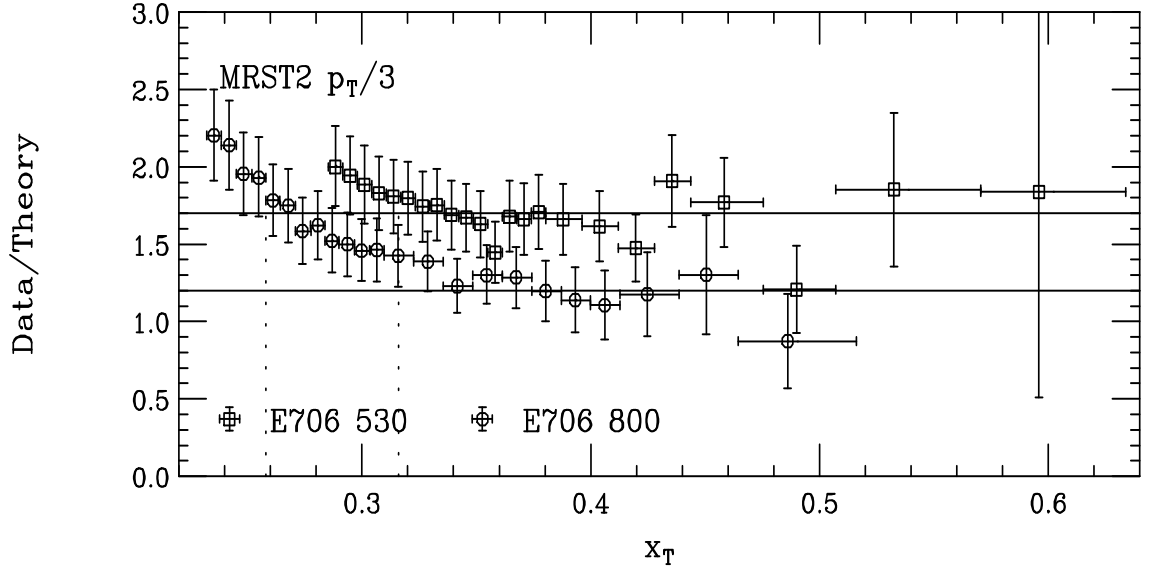


Figure 11: Same as Fig. 10, but for E706 $[10] \pi^0$ data. The dotted vertical lines correspond to $p_T = 5$ GeV/c for the two E706 energies. Only data points with $p_T > 4.5$ GeV are kept to avoid the use of too small factorization scales in the NLO predictions.

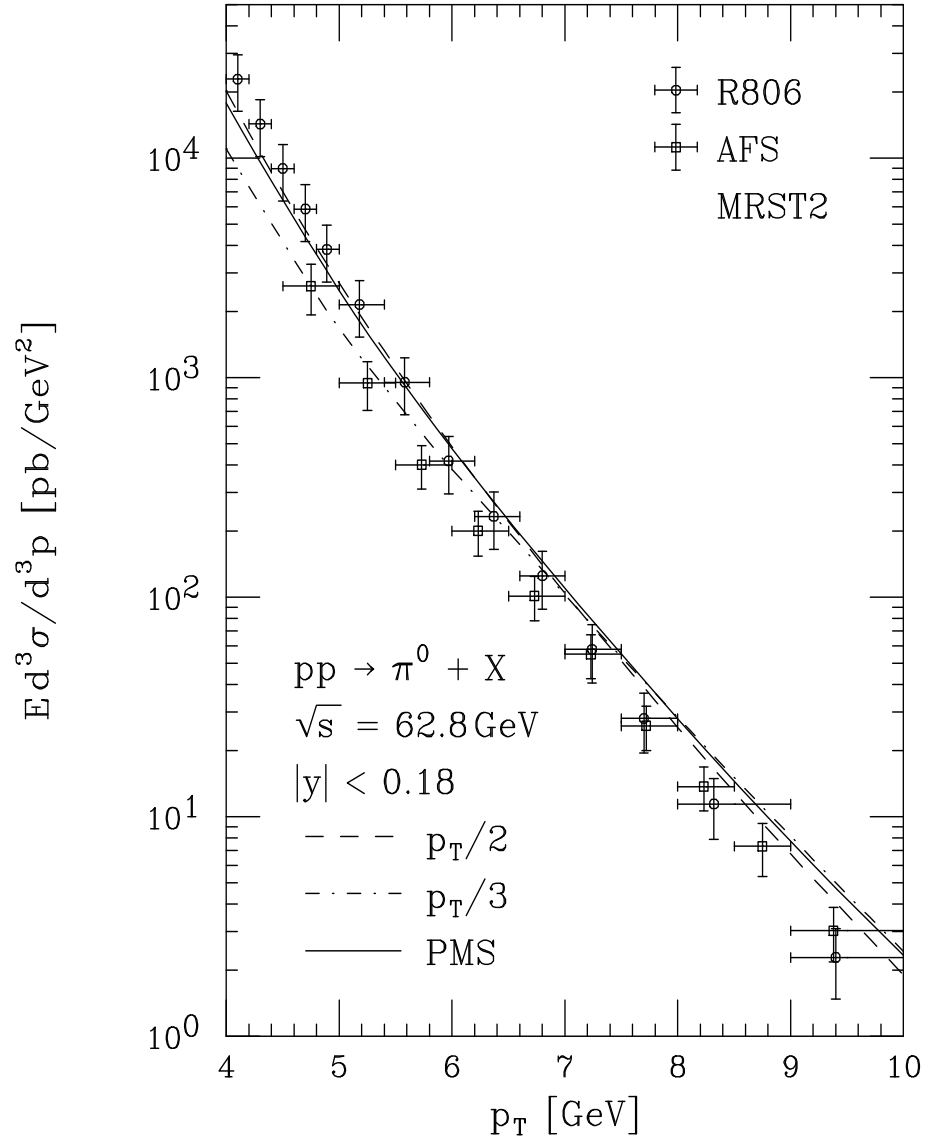


Figure 12: Comparison of R806 [21] and AFS [22] π^0 data with NLO predictions based on the MRST2 [5] parton densities.

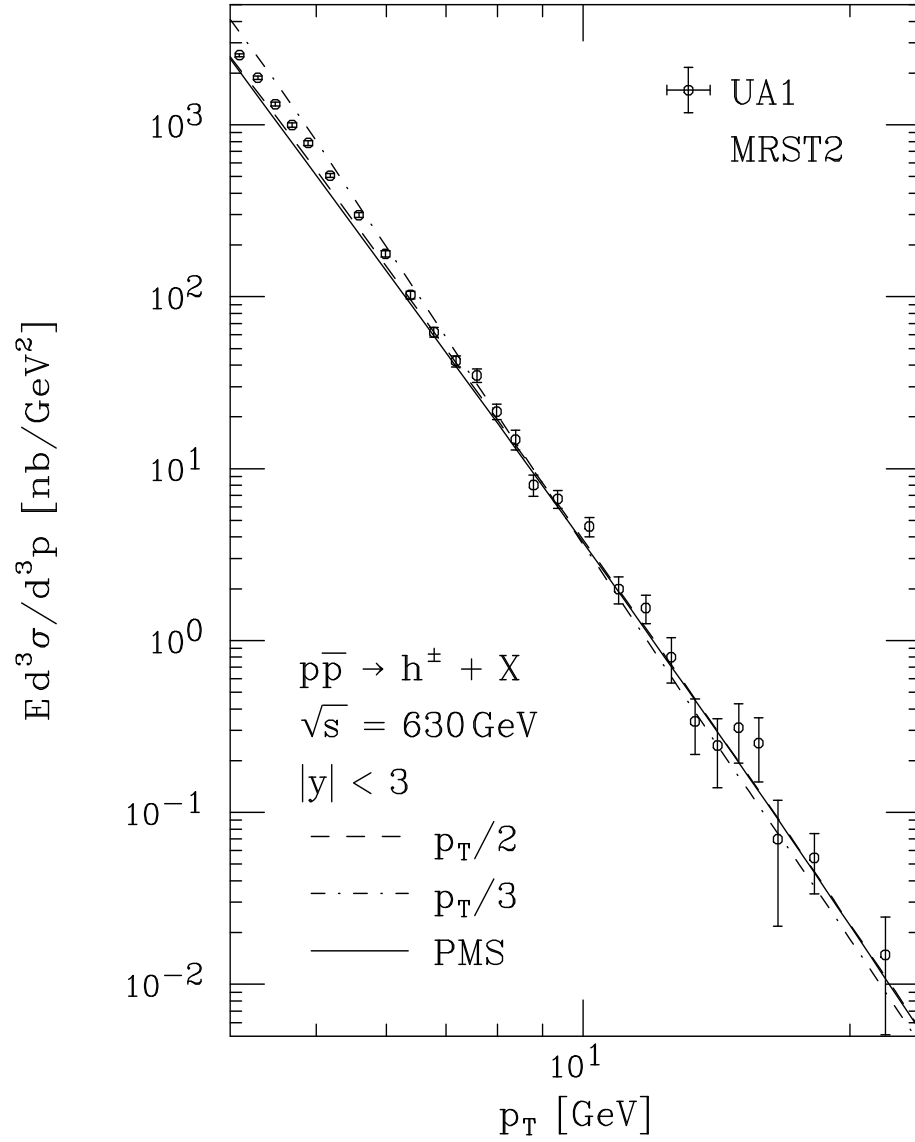


Figure 13: Comparison of UA1 [16] charged-hadron data with NLO predictions based on the MRST2 [5] parton densities.